Supporting Information for

Post-fabrication annealing effects on Insulator-Metal Transitions in VO$_2$ thin-film devices

Servin Rathi[1], In-yeal Lee[1], Jin-Hyung Park[1], Bong-Jun Kim[2], Hyun-Tak Kim[2,3], and Gil-Ho Kim[1a)*

[1]School of Electronic and Electrical Engineering and Sungkyunkwan Advanced Institute of Nanotechnology (SAINT), Sungkyunkwan University, Suwon 440-746, Korea

[2]Metal-Insulator Transition Creative Research Center, ETRI, Daejeon 305-700, Korea

[3]School of Advanced Device Technology, Korean University of Science & Technology, Daejeon 305-700, Korea
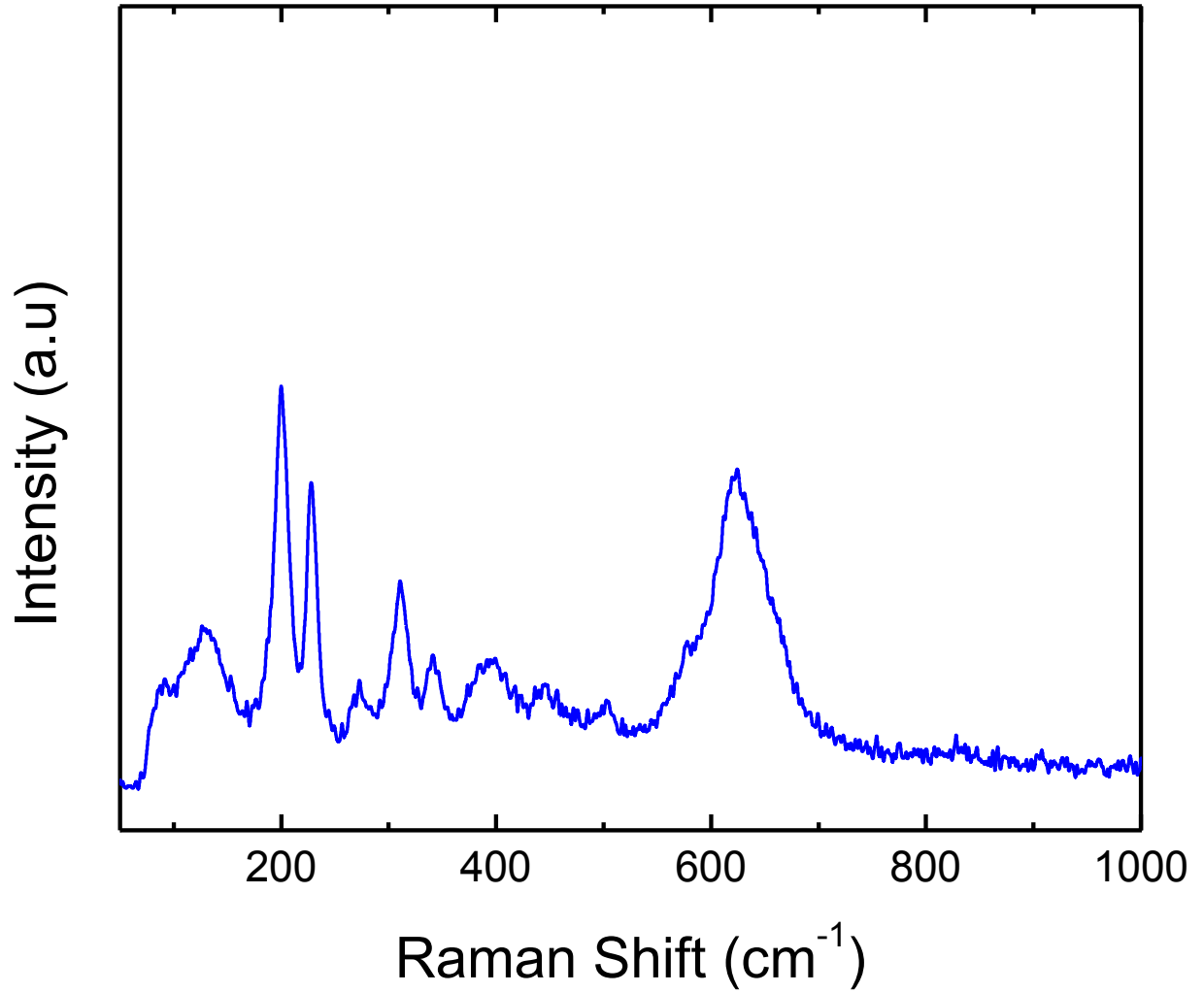
[a]Electronic mail: ghkim@skku.edu

Figure S1. Raman spectra of a VO_2 thin film.

The peaks in Raman spectra in Figure S1 are identified at 197(A_g), 227(A_g), 264(B_g), 311(B_g), 343(B_g), 396(A_g), 443(B_g), 614(A_g) cm^{-1}. The low-frequency phonons (197(A_g) and 227(A_g)) correspond to V-V lattice motion and other distinguishable peaks relate to V-O bonding.[1] These Raman-active modes are the clear signature of good quality VO_2 thin film.
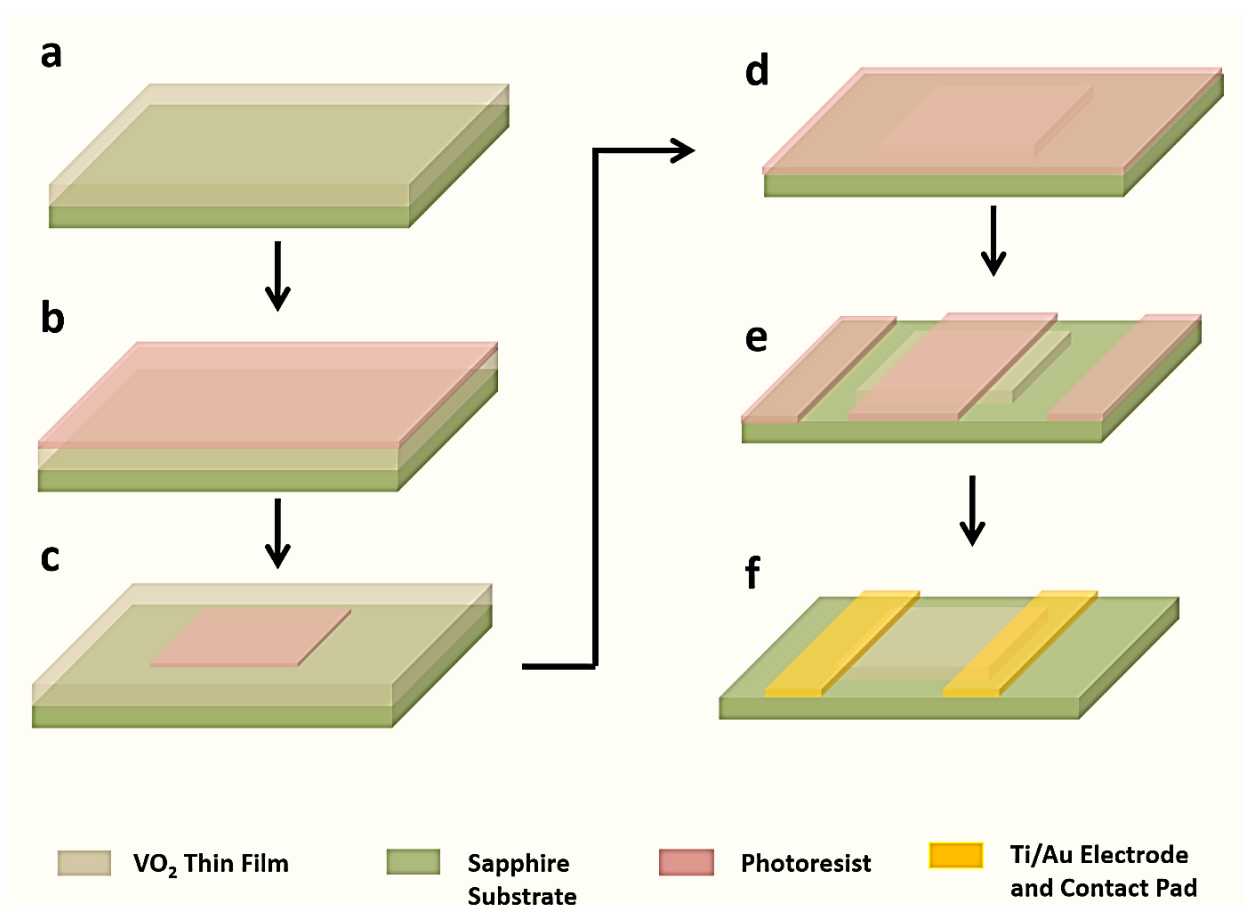
Figure S2. (a-f) Steps to fabricate device from VO_2 thin film on sapphire substrate.

The VO_2 thin film grown on sapphire substrate for good quality thin films (Figure S2 (a)) are first coated with UV photoresist (PR) using a spin coater (Figure S2 (b)) and then using an appropriate mask the etching pattern are developed on the thin-film (Figure S2 (c)). The exposed thin film is then etched using plasma etching consisting of CF_4 and O_2 gases and the PR is dissolved in acetone. Then PR is coated once again (Figure S2 (d)) and the electrode mask is used for patterning the electrodes (Figure S2 (e)). The developed pattern is then put in e-beam

metal deposition chamber and Ti/Au (10/150 nm) is deposited. The pattern is then lift-off in acetone (Figure S2 (f)) and ready for further measurement and analysis.
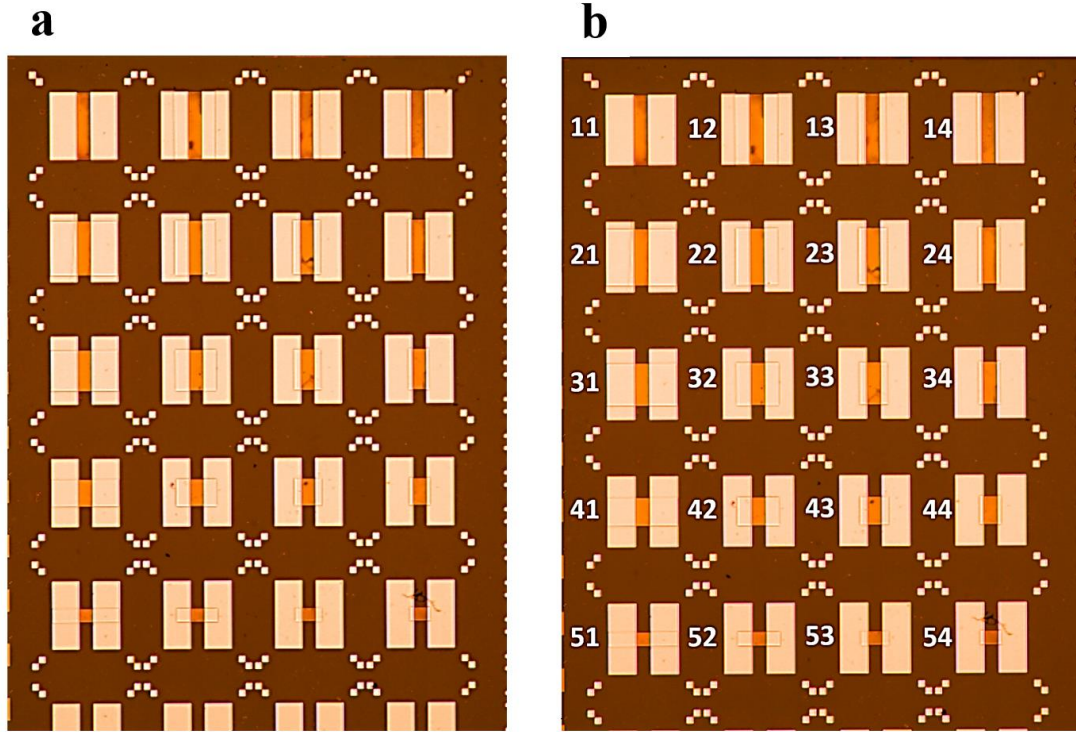

Figure S3. Fabricated devices (false color image) for two terminal measurement, **a**, left image shows the devices, **b**, right one denotes the numbering sequence to identify the devices. The metal contact pad length and width is 500 and 200 μm respectively. The gap between the electrodes is fixed at 200 μm while the width of the thin film varies from 500, 400, 300, 200, 100, 50 μm from top to bottom.
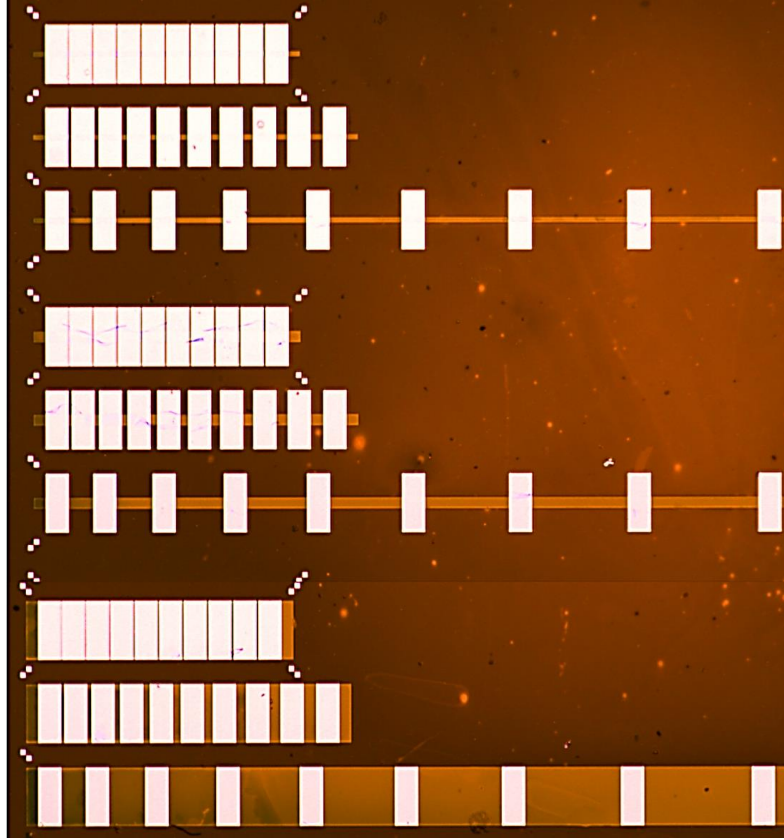
Figure S4. Fabricated device (false color) for Transmission Line Measurement (TLM). The channel widths from bottom to top are 500, 100 and 50 μm while the gap between the electrodes from left to right varies from 200, 300, …1000 μm for first strip, 20, 30, …..100 μm for the second and 2, 3, …..10 μm for the third line for each group.

Figure S3 and S4 show the fabricated devices used for two-terminal and Transmission line measurement. The dark color horizontal strips patterned by the vertical strips represent thin film and metal contact respectively in figure S3. While in figure S4 long horizontal strips of different width are patterned by the vertical metal contacts of various gap between the consecutive contacts. This variation in length is used to plot the resistance versus length curve from which

the contact and sheet resistance of the thin film can be calculated. Further, thin film devices of various thickness, Figure S5, have been fabricated and tested for the experimental results.
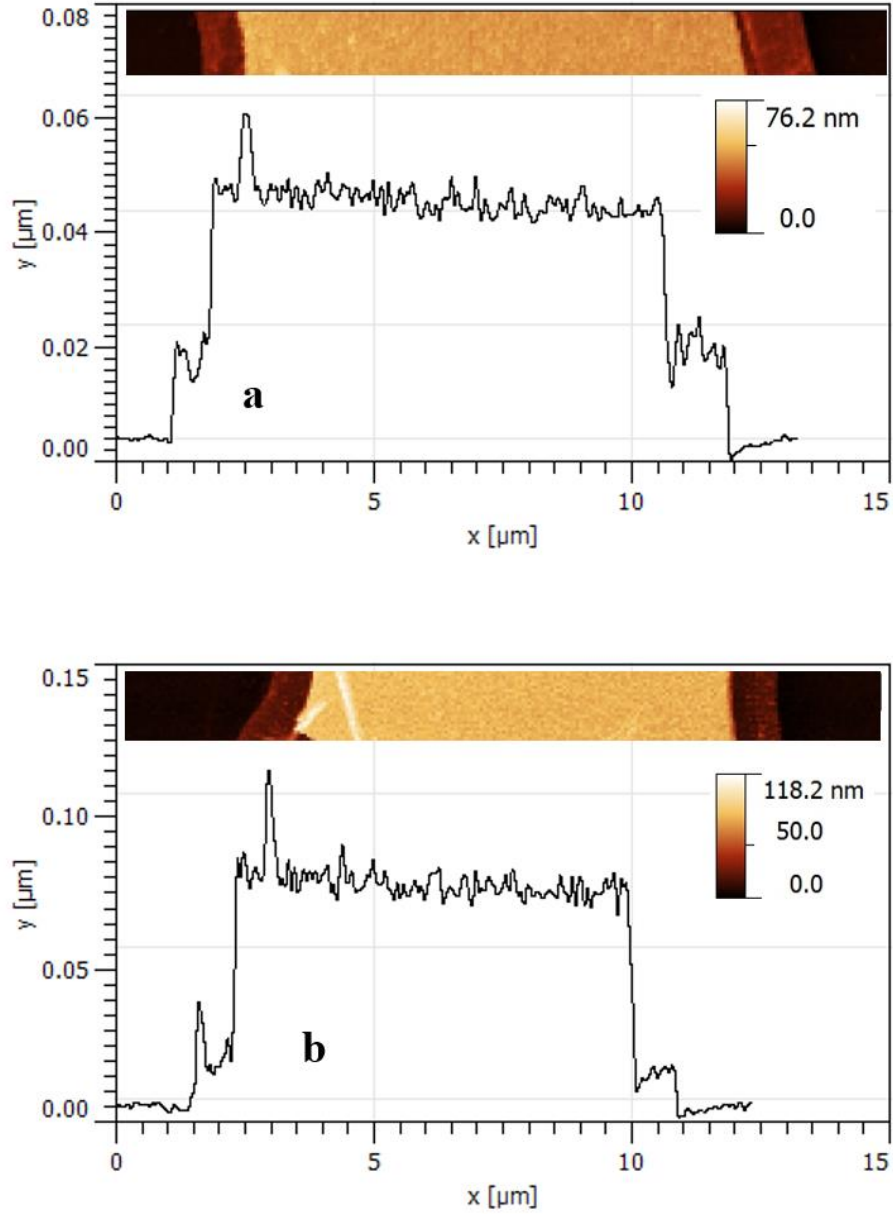

Figure S5. The deposited VO$_2$ thin films of various thickness were deposited **a.** AFM profile of showing 50 nm thick film while **b.** shows thin film of 85 nm thickness.
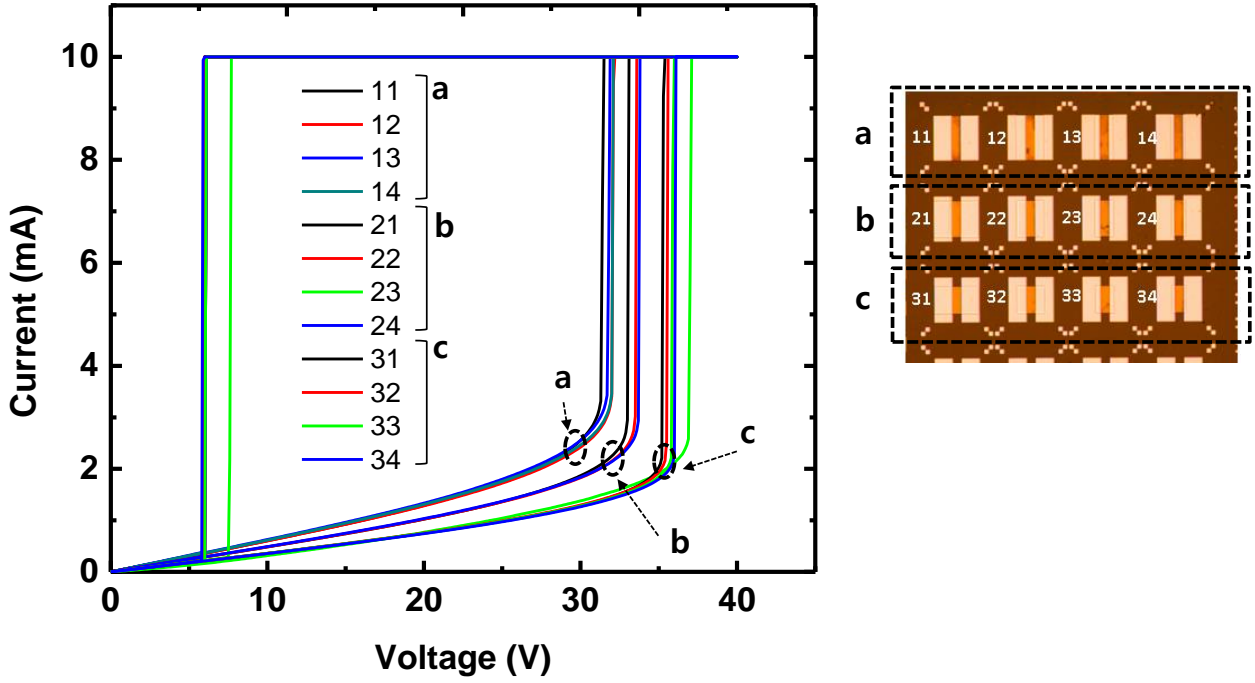
Figure S6. Dual sweep I-V characteristic of one of the device group at 55 °C. The negligible variations observed in the devices of similar channel length and width arise from the small variation in the contact or thin film resistances.

Figure. S6 and S7 show the variation in threshold voltage with the channel width. As the width gets shorter, device resistance increase thus the threshold voltage also increases.
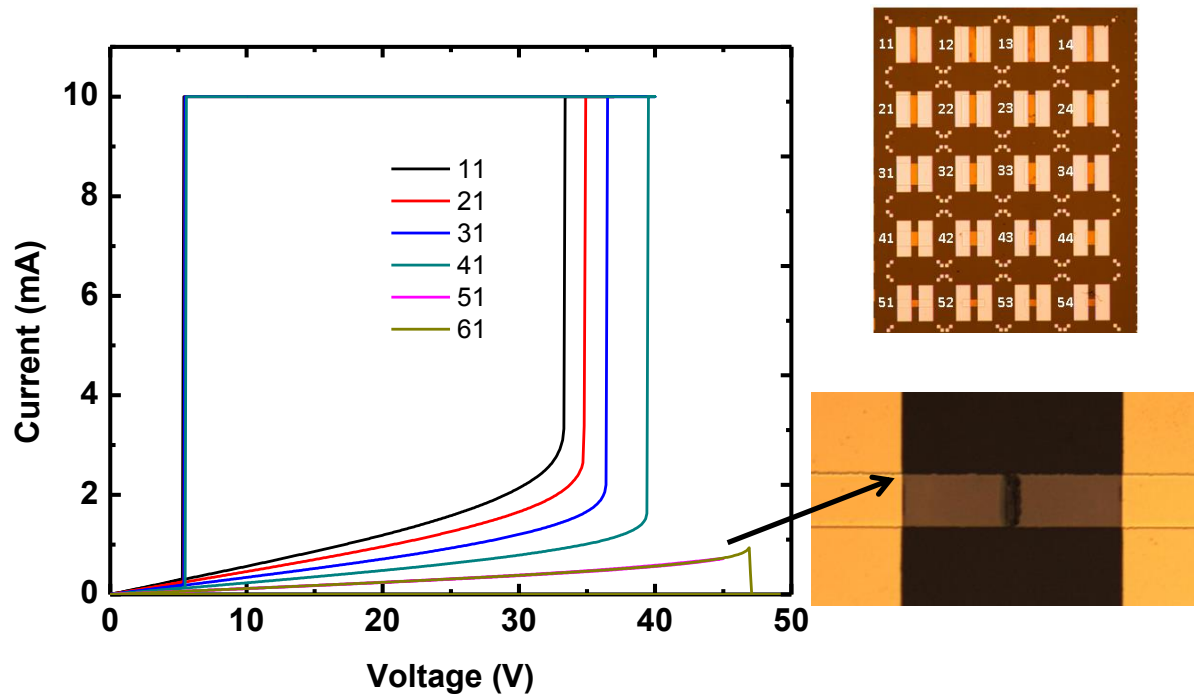
Figure S7. Dual sweep I-V characteristic of one of the devices at 55 ^{o}C for same channel length but different channel width. The channel width varies from 500, 400... 100 μm from top to bottom. The inset figures on the upper right show the measured device labels while one on the lower right show the optical image of the burned device.
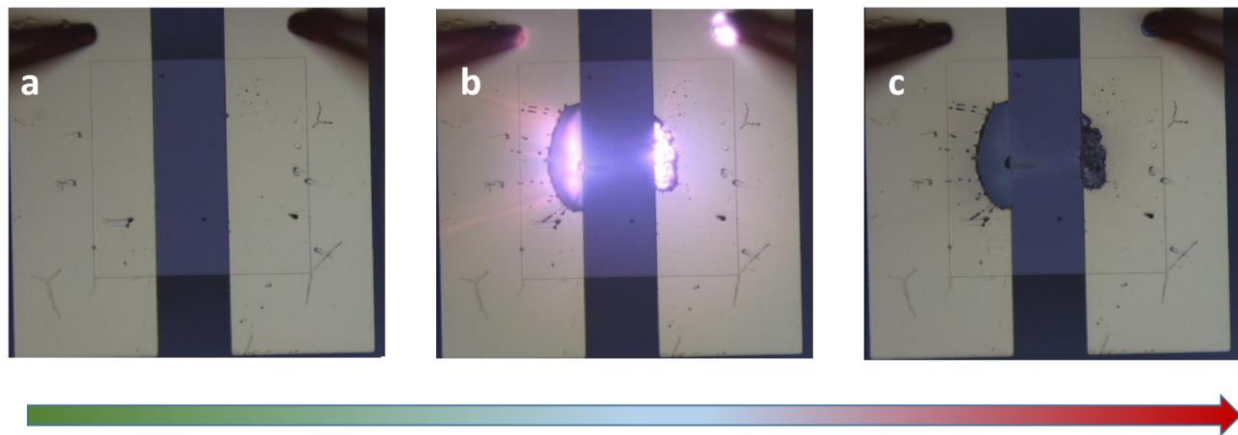

Figure S8. Images of the device before, during and after burning out in the course of voltage sweeping from low to high.

As seen from the figure S7 (inset) and S8, a voltage higher than a critical value results in the thin film burn-out. This has also been shown in the video clip. However, for voltages below burn-out limit, it can be seen that instead of transition in whole channel width, only a small part of the width is converted to metal from insulator, as can be seen from the contrast color (metal-filament) in figure S9 and the related video clip. The observed contrast is due to the variation in optical transmission properties where the metallic part has lower transmission value than the insulating regions. Similar studies based on optical transmission properties have been pursued by other research groups.[2]
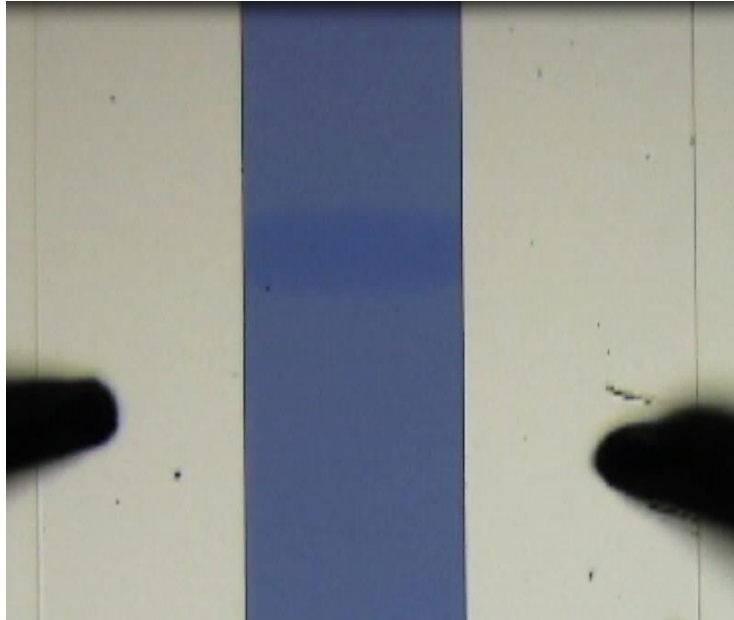

Figure S9. Images of the device after the metal-insulator transition. A contrast channel (metal filament) can be seen in the middle of the channel indicating the metallic part.

It was found that the filament width have negligible dependence on the annealing conditions, as all the devices in the metallic state shows similar resistance. However, the width of filament shows dependence on the compliance current and increases with the current value as seen in

figure S10. Considering the power limitation of the Keithely measurement system, a device with 20 µm length was tested for the filament-current dependence on compliance-level, as devices with wider gaps need high power to flow current at high compliance-level.
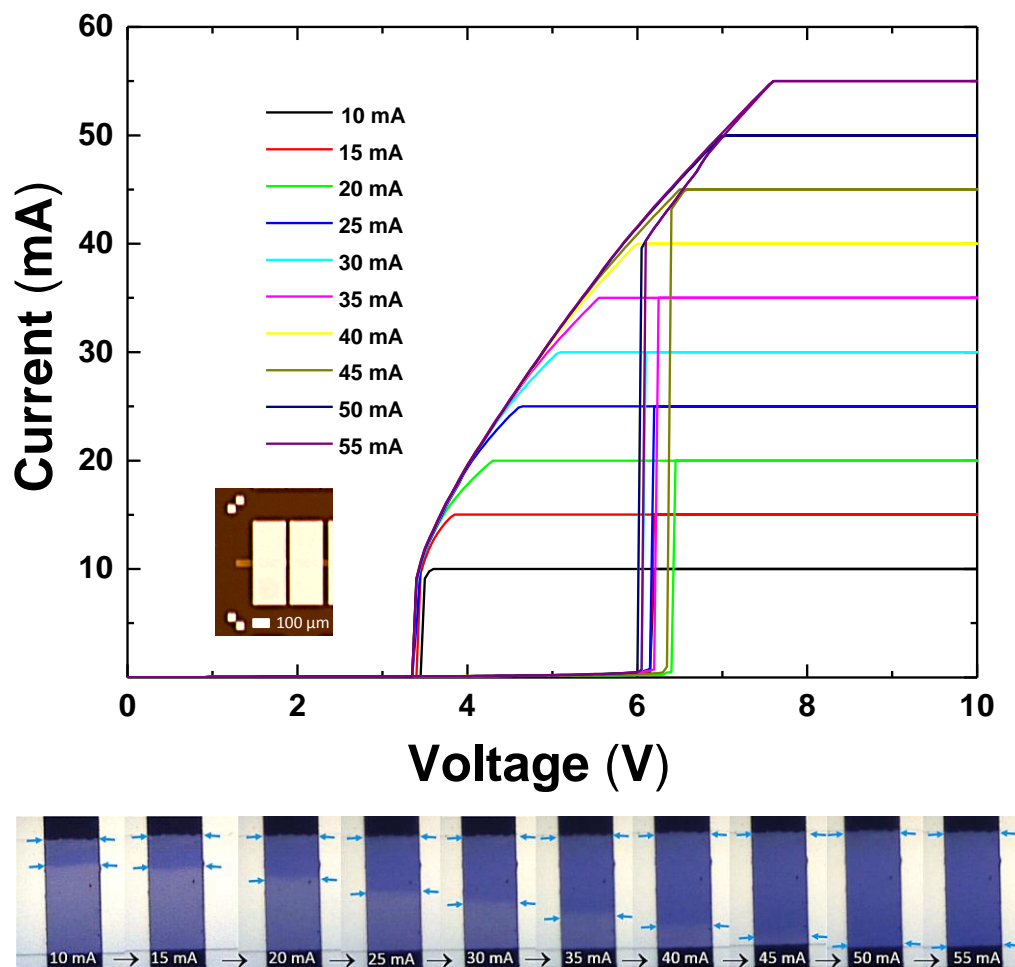

Figure S10. Voltage induced transition for different compliance current at 50 $^\text{o}$C. Inset on the bottom shows the variation in the metal-filament width with the compliance current.
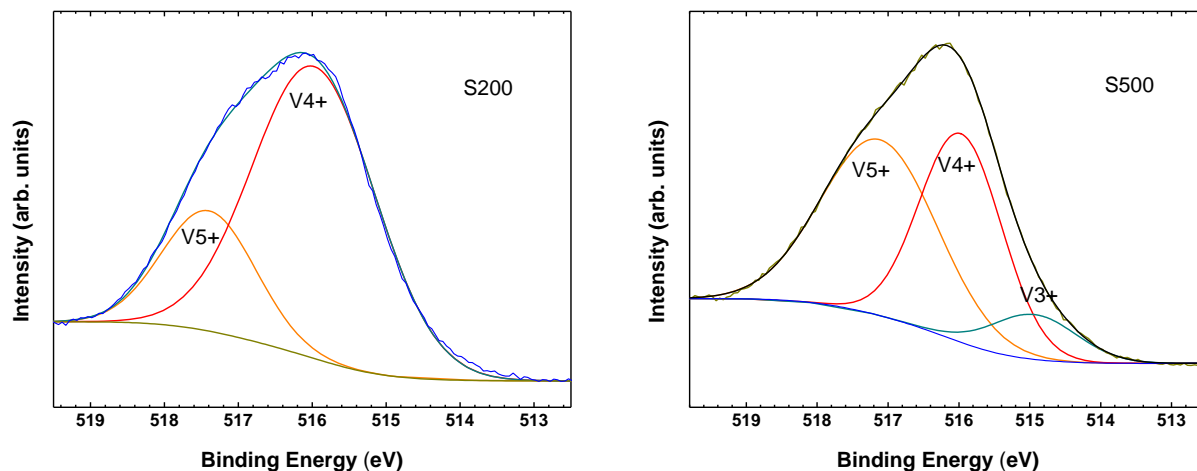
Figure S11. High-resolution scan of V 2p$_{3/2}$ XPS peak, fitted and resolved via deconvolution. (a) S200 sample, where deconvolution gives two peaks corresponding to +5 and +4 valence states. (b) S500 sample, where three peaks corresponding to +5, +4 and +3 valence states are obtained. The fitting is carried out after subtraction of the Shirley baseline background.

Information from XPS data, in particular V 2p$_{3/2}$ peak can give a qualitative information regarding the fraction of the mix valence states in the thin-film. Figure S11 shows XPS fitted curves where peaks attributed to +5, +4 and +3 valence states can be detected by their binding energies which increases with the oxidation state.[3,4] It can be seen that the after annealing at 500 ^{o}C, fraction of +4 decreases while +3 appears, which indicates the reducing effect of annealing process.
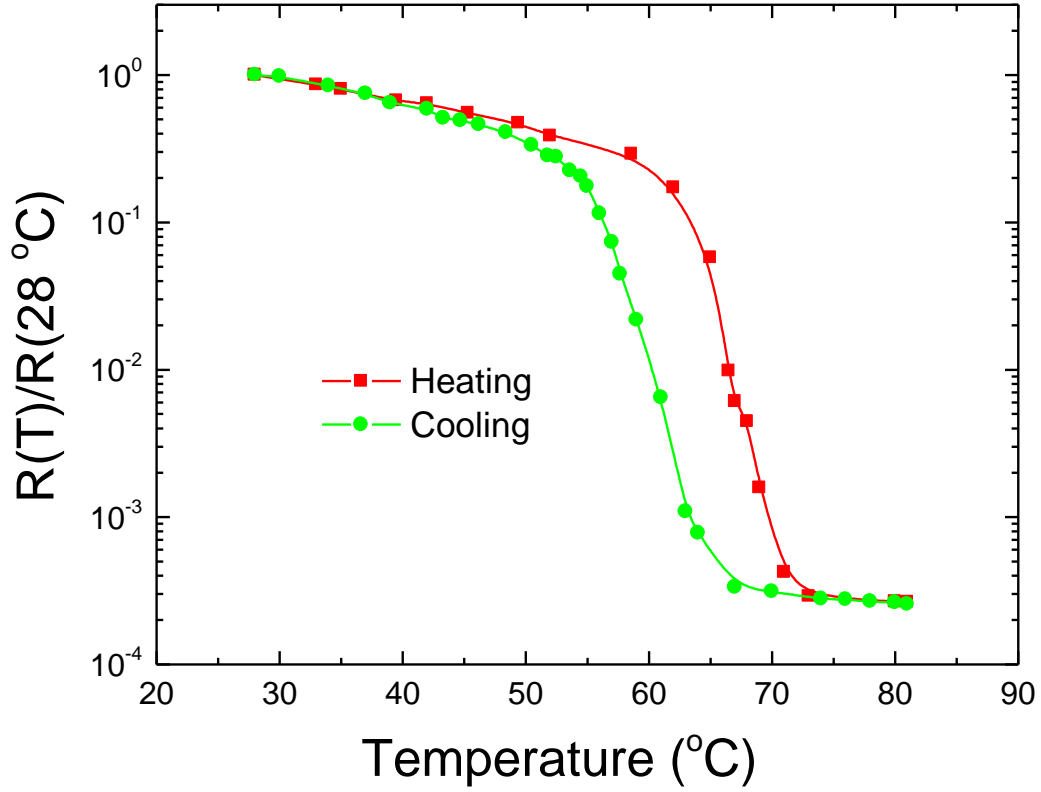
Figure S12. Resistance versus temperature measurement for both heating and cooling.

An R-T curve is plotted in figure S12 showing the variation in resistance with temperature. It can be seen that a well-defined hysteresis like in the voltage-induced transition also forms during the cooling cycle. In order to measure the transition temperature, a first-order derivative is taken for the heating curve, the peak of this curve would give the transition temperature of that device.
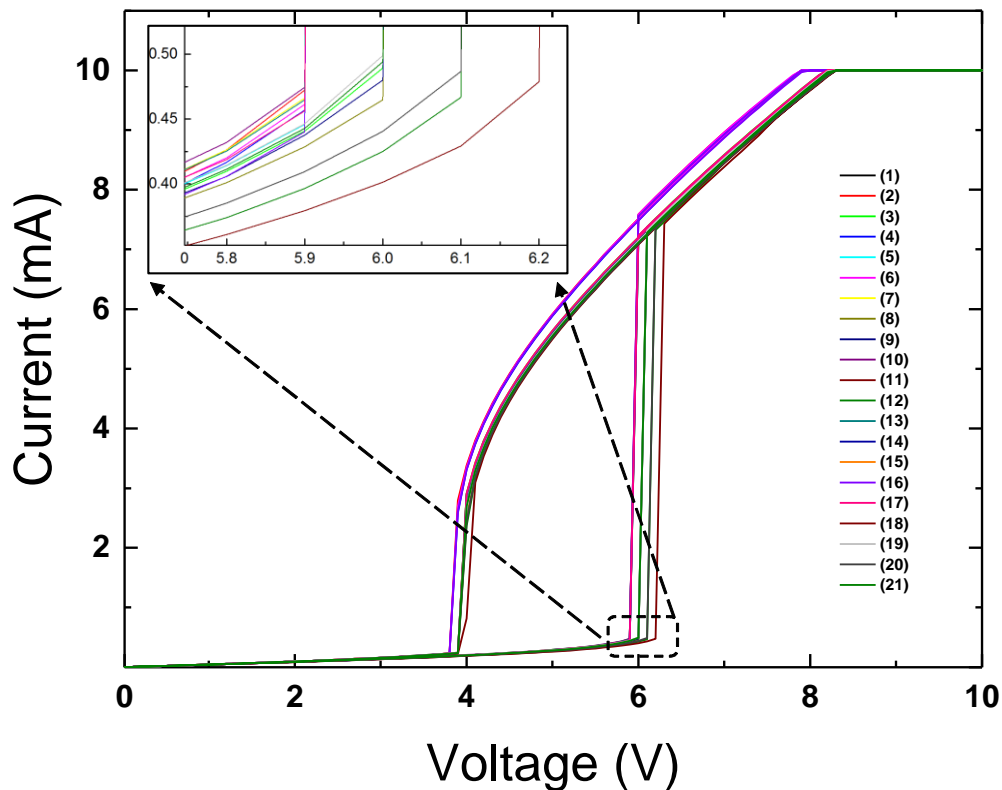
Figure S13. Random fluctuations in the transition voltage for several sweeping cycles.

During the course of repeated voltage sweeping, random fluctuations in the transition voltage have been observed as shown in figure S13. The cause of these variations could be the random current path after every transition cycle. The hysteresis behavior of VO_2 material and failure of thin-film's grains to fully recover to their original properties could also lead to minor variation in the thin-film resistance after every transition. However, to avoid any false value in the measurements, the I-V sweeps several times until a stable point is sufficiently reproducible.
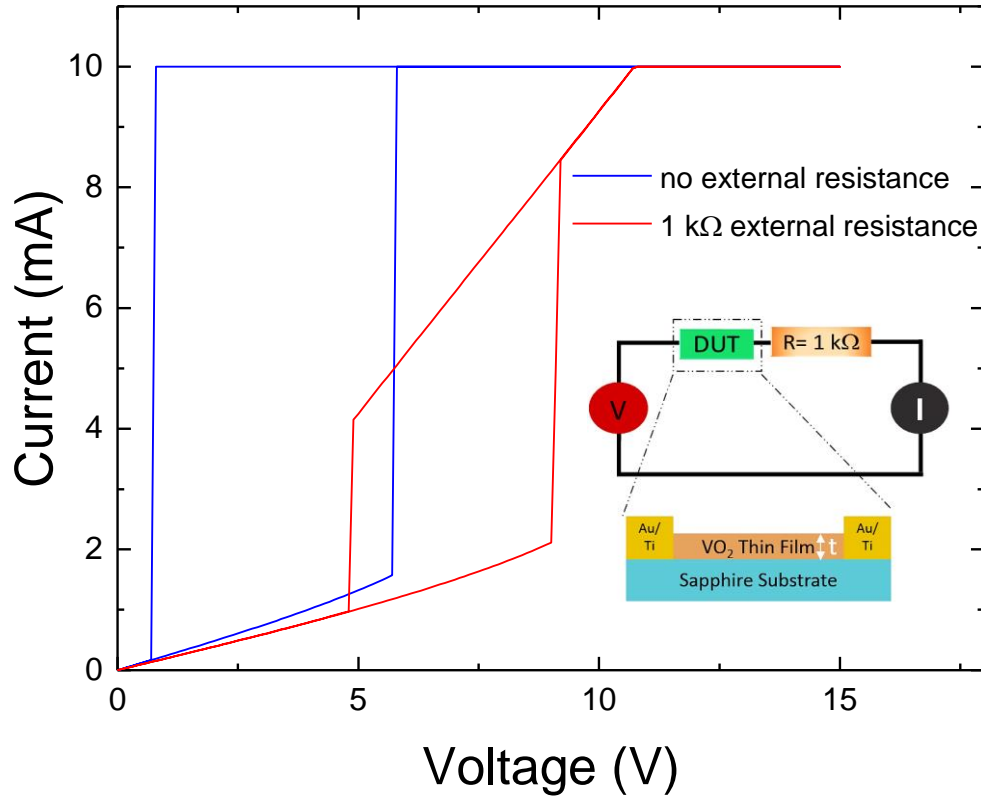
Figure S14. Measurement of metallic state resistance with 1 kΩ resistance connected in series.

The introduction of external resistance in the measurement circuit could enable to measure the resistance in the metallic phase which would otherwise can only be obtained from thermal measurement. It can be seen in the figure S14 that adding a resistor of 1kΩ leads to a shift in transition voltage for both forward and backward sweep. This can be explained due to extra potential drop across resistance which required an additional voltage to achieve the transition point. Although, transition points are shifted but the device shows similar hysteresis.

REFERENCES

(1) Kim, H, T.; Chae B. G.; Youn, D. H.; Kim G.; Kang, K. Y.; Lee,S. J.; Kim, K.; Lim, Y. S. Raman Study of Electric-Feld-Induced First-Order Metal-Insulator Transition in VO$_2$-based Devices. *Appl. Phys. Lett.* **2005**, *86*, 242101.

(2) Kumar, S.; Pickett, M. D.; Strachan, J. P.; Gibson, G.; Nishi, Y.; Williams, R.S. Local Temperature Redistribution and Structural Transition During Joule-Heating-Driven Conductance Switching in VO$_2$. *Adv.Mater.* **2013**, *25*, 6128-6132.

(3) Gopalakrishnan, G.; Ramanathan, S. Compositional and Metal-insulator Transition Characteristics of Sputtered Vanadium Oxide Thin Films on Vttria-stabilized Zirconia. *J Mater Sci*. **2011,** 46, 5768–577.

(4) Yang, Z.; Ko, C.; Ramanathan. S. Metal-insulator Transition Characteristics of VO$_2$ Thin Films Grown on Ge(100) Single Crystals. *J. Appl. Phys.* **2010**, 108, 073708.